

## PRECISE WAVELENGTH MEASUREMENTS OF FORBIDDEN TRANSITIONS IN HIGHLY CHARGED ARGON AND KRYPTON IONS

I. N. Draganić<sup>1,2</sup>, J. R. Crespo López-Urrutia<sup>2</sup>, R. Soria<sup>2</sup>, R. DuBois<sup>3</sup>, S. Fritzsche<sup>4</sup>, Y. Zou<sup>5</sup> and J. Ullrich<sup>2</sup>

<sup>1</sup>Vinča Institute of Nuclear Sciences, Laboratory of Physics (010), P.O. Box 522, 11001 Belgrade, Serbia and Montenegro

<sup>2</sup>Max-Planck Institut für Kernphysik, Saupfercheckweg 1, D-69117 Heidelberg, Germany

<sup>3</sup>University of Missouri-Rolla, Physics Building, Rolla, MO 65409-0640, USA

<sup>4</sup>Department of Physics, University of Kassel, Heinrich-Plett-St. 40, D-34132 Kassel, Germany

<sup>5</sup>Applied Ion Beam Physics Lab, Fudan University, Shanghai 200433, P.R. China

**Abstract** – We present the results of an experimental study of magnetic dipole (M1) transitions in highly charged ions of argon (Ar X, Ar XI, Ar XIV, Ar XV) and krypton (Kr XIX, Kr XXIII) in this paper. The wavelengths of these forbidden transitions, in the visible and near UV ranges, were determined with unprecedented accuracies up to sub ppm level using an Electron Beam Ion Trap as a favorable source. Our wavelength measurements represent benchmarks and a challenge for the present-day atomic structure theory.

### 1. INTRODUCTION

The sun, and in particular the solar corona, has provided a fantastic source of basic atomic information. Already in 1868, for example, Helium was discovered by Lockyer in the spectrum of solar corona [1], more than 25 years before it was found and eventually isolated on the earth. Forbidden transitions, which play a vital role in the temperature and density diagnostics of both terrestrial [2] and astrophysical plasmas [3], were first identified in the solar corona by Edlén [4]. This discovery led to a re-evaluation and to a drastic recalibration of the temperature of the solar corona from six thousand degrees to two million degrees [5]. The solar corona acts as a unique laboratory where atomic physics concepts can be both used and tested. However, the depth of understanding of any astrophysical object ultimately rests on the quality of laboratory based atomic data. For example, the forbidden line identifications by Edlén [4] were based on very accurate energy level data for the elements in question. In more recent years, the major advances in using spectra lines, and in particular forbidden lines, in the analysis of astrophysical plasmas have been successfully transferred to the diagnostics of fusion plasmas, e.g. in Tokamak devices. The element abundances here are more defined by the requirements of needing spectral lines for diagnostics of the plasma, while at the same time keeping the concentrations low so as not to disrupt the power balance due to radiation losses. Argon and krypton are often chosen for injection into Tokamaks, and hence are useful diagnostic elements. Again, high quality atomic data are needed to give confidence to the diagnostic methods. Apart from the applications to plasma diagnostics, the precise wavelength measurements of magnetic dipole transitions (M1) arising between levels of the ground configurations of few-electron highly charged ions can provide sensitive probes for *ab initio* and semi-empirical theoretical atomic structure calculations [6-12]. At

present, there are no calculations that reproduce the wavelengths, such as those for M1 transitions, at the level of accuracy to be described in this paper. Hence, the results presented in this work challenge modern methods for calculating atomic structure. Moreover, our data will make significant impact on the elaboration of atomic data bases.

In this work, we measured the wavelengths of the M1 transitions of Ar X  $2s^2 2p^5 \ ^2P_{3/2} - \ ^2P_{1/2}$ , Ar XI  $2s^2 2p^4 \ ^3P_2 - \ ^3P_1$ , Ar XIV  $2s^2 2p \ ^2P_{1/2} - \ ^2P_{3/2}$ , Ar XV  $2s 2p \ ^3P_1 - \ ^3P_2$ , Kr XIX  $3p^5 3d^1 \ ^3P_1 - \ ^3P_2$  and Kr XXIII  $3p^2 \ ^3P_1 - \ ^3P_2$ . These measurements were done exploiting the very favourable conditions offered by an Electron Beam Ion Trap, EBIT, for high-resolution spectroscopy studies on highly charged ions. A good general reference to EBITs and their applications to atomic physics can be found in [13]. The argon lines have been previously studied in a number of works e.g. iso-electronic studies by Edlén in 1982 [14] and 1983 [12,15], and EBIT studies, the most recent being by Bieber *et al.* [16]. The krypton lines under investigation here have been the subject of a number of Tokamak and EBIT studies in recent years. Earlier work on krypton, mainly Tokamak studies, is summarized in a set of data tables [17], and examples of more recent EBIT works can be found in [18] and [19]. In this work, we developed a new approach for precise wavelength determination, and obtained accuracies up to sub-ppm level. Error sources from statistics, calibration line uncertainties, cut-off of high order of calibration functions, collision and Doppler broadening, Zeeman and Stark effects, as well as CCD-size, flaw and temperature drifts during the measurements were considered.

### 2. EXPERIMENTAL SETUP

The experiment was performed on the FreEBIT (Now H-EBIT at MPI-K Heidelberg) at the University of Freiburg. The superconducting magnet coils were operated at a current of 50 A, which corresponds to a magnetic induction of  $B=5.25$  T in the trap region. The electron beam energies were  $E_{\text{beam}}=1010$  eV for the argon and  $E_{\text{beam}}=1200$  eV for the krypton measurements, with the beam currents of 45-50 mA for both cases. For these experiments the length of the ion trap was chosen to be 40 mm and the axial potential depth was  $U=100$  V. The trap region was dumped every 10 seconds using a 150 V, 10 ms pulse to avoid the accumulation of heavy ions like Ba and W which arise as contaminants from the electron gun. Argon or krypton gas is introduced into the trap region through a gas injector system. The gas pressure

was around  $1 \times 10^{-7}$  mbar in the Ar X and Ar XI measurements, and lower than  $1 \times 10^{-9}$  mbar for Ar XIV and Ar XV and all the krypton measurements. The vacuum in the trap was in the range of  $1 \times 10^{-9}$  to  $1 \times 10^{-12}$  mbar. All working and adjustment parameters of EBIT were stable with the time during measurements.

Photons in the visible and near UV wavelength range were coupled from the trap through 2 pairs of quartz lenses to the entrance slit of a JY TRIAX 550 spectrograph equipped with a cryogenic CCD camera (2000x800 pixels on a 30x12 mm<sup>2</sup> chip). X-rays from the trap were monitored by a high-purity Ge detector (IGLET). The entrance slit of the spectrograph was set to 50  $\mu$ m as a compromise for line intensity and resolution. We chose the exposure time for each measurement such that the recorded spectral lines from the trapped ions contained about 1500 counts for weak lines and 100 000 counts for strong lines. A typical spectrum is shown in Fig.1.

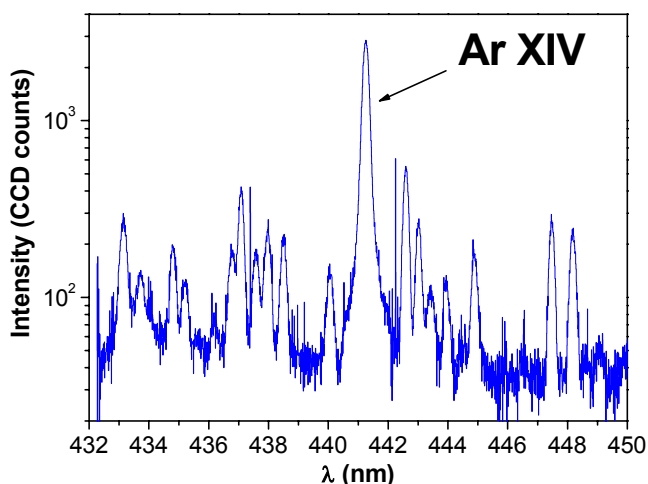


Fig.1: An example of a typical line shape for a forbidden transition as measured in this paper.

Throughout the measurements, the signal to noise ratio was kept at around 100. The calibration spectra were recorded before and after each exposure. For all calibration spectra measurements, a diffuse reflector (illuminated with pencil spectral lamps) was placed at the position of the first real image of the trap, just outside the vacuum quartz window. Afterwards, the grating was slightly rotated. A new exposure, with its corresponding calibrations, was then recorded. The entire process was repeated as many as thirty times. In this way, the statistical limitations posed by too few pixels illuminated across the width of a spectral line, and the possible flaws of CCD pixels were overcome, and the sampling of the line profile was improved by recording several hundred data points for each line profile.

### 3. RESULTS

Each spectrum was evaluated by fitting individual Gaussian functions to the calibration lines and using a least-square-algorithm to obtain a second-degree polynomial for the dispersion function. Since the deviation from linear dispersion for this type of spectrograph is small, a quadratic function already provides a very good approximation to the real dispersion. The calibration procedure was repeated at about 30 different grating positions. Hence, any non-linearity in the detector response for individual pixels became

negligible. The effect of deviations of the line profile from an ideal Gaussian shape was checked by varying the intervals around the line center for the fitting procedure. This was done in order to take into account the background, scattered light, Zeeman effect, coma

aberration and so on, which could affect the line shape. Such a test leads to average centroid shifts of about 0.004 pixel, or  $3.5 \cdot 10^{-5}$  nm. In this work we neglected the line wavelength shift caused by Stark effect, below  $10^{-7}$  nm from our estimation, by collisions,  $10^{-12}$  nm, and by Paschen-Back effect,  $10^{-6}$  nm. Other possible sources of systematic deviations like temperature drift etc. are ruled out by our calibration procedure. The main error sources together with their contributions to the final uncertainties are listed in the Table 1.

Source	Contributions to wavelength uncertainty ( $10^{-4}$ nm)					
	Ar <sup>9+</sup>	Ar <sup>10+</sup>	Ar <sup>13+</sup>	Ar <sup>14+</sup>	Kr <sup>18+</sup>	Kr <sup>22+</sup>
Line centroid	1.1	0.9	0.6	3.3	2.3	0.5
Standard deviation of dispersion function	1.1	1.6	0.2	0.9	3.6	3.1
Calibration wavelength uncertainty	0.4	10	0.1	0.7	0.8	0.2
Calibration systematic uncertainty	0.3	0.1	0.2	0.5	0.6	0.1
Total	2	12	1	5	6	3

Table 1: The list of the main error sources and their contributions to the final uncertainties of the wavelengths.

All random uncertainties (the line centroid errors, standard deviations of wavelength calibration function) have been calculated as a “root sum of squares”, whereas systematic calibration errors and uncertainties from the calibration lines have been added linearly.

In this work, a series of multi-configuration Dirac-Fock (MCDF) computations have been carried out for both argon and krypton ions. The effects from the core-polarization and core-core correlations were considered and compared with the zero order approximation. Both the experimental and theoretical results from this and other works are listed in Table 2. As can be seen in Table 2 in comparison with other experiments, our results for Ar<sup>9+</sup>, Kr<sup>18+</sup> and Kr<sup>22+</sup> are almost two orders of magnitude more accurate than the previous most accurate data [24,19,31-32]. Our Ar<sup>9+</sup> and Kr<sup>22+</sup> results are in accord with the data from the previous experiments [24,31] within error bars. The result for Kr<sup>18+</sup> does not agree with the data from the references [19,32,33], being different by 0.13 nm. For Ar<sup>10+</sup>, Ar<sup>13+</sup>, and Ar<sup>14+</sup>, Bieber et al has done very precise experiments [16]. Still, in our work, the accuracies have been improved by factors of five to thirty. At this accuracy level, we found discrepancies for the lines of Ar<sup>13+</sup> and Ar<sup>14+</sup>, between our results and theirs, 0.0059 nm for Ar<sup>13+</sup> and 0.015 nm for Ar<sup>14+</sup>.

Ion	Transition	Experimental wavelength ( nm)		Theoretical wavelength (nm)	
		In air		In air	
		This work	Others	This work	Others
Ar <sup>+9</sup> (F-like)	2s <sup>2</sup> 2p <sup>5</sup> <sup>2</sup> P <sub>3/2</sub> – <sup>2</sup> P <sub>1/2</sub>	553.3265±0.0002	553.34±0.02[24]	554.75 <sup>1</sup> 554.20 <sup>2</sup> 553.80 <sup>3</sup>	553.339 [20]
Ar <sup>+10</sup> (O-like)	2s <sup>2</sup> 2p <sup>4</sup> <sup>3</sup> P <sub>2</sub> – <sup>3</sup> P <sub>1</sub>	691.6878±0.0012	691.686±0.006[16] 691.7[25] 691.72[26]	693.24 <sup>1</sup> 692.86 <sup>2</sup> 692.28 <sup>3</sup>	687.3[21] 691.8[22] 691.6[15]
Ar <sup>+13</sup> (B-like)	2s <sup>2</sup> 2p <sup>2</sup> P <sub>1/2</sub> – <sup>2</sup> P <sub>3/2</sub>	441.2559±0.0001 *441.2563±0.0004	441.250±0.003[16] 441.26±0.02[27] 441.132±0.2[28] 441.32±0.2[29] 440.0±2[30]		438.7[21] 442.1[6] 441.2[7] 441.1[8] 441.65[34] 441.32[15]
Ar <sup>+14</sup> (Be-like)	2s 2p <sup>3</sup> P <sub>1</sub> – <sup>3</sup> P <sub>2</sub>	594.3880±0.0005	594.373±0.004[16] 594.4[9] 595.5±2[30]	596.46 <sup>1</sup> 594.79 <sup>2</sup>	597.9[21] 594.5[10] 594.0[11] 594.37[12]
Kr <sup>+18</sup> (Ar-like)	3p <sup>5</sup> 3d <sup>1</sup> <sup>3</sup> P <sub>1</sub> – <sup>3</sup> P <sub>2</sub>	402.7143±0.0006	402.69[23] 402.58±0.05 [19,32,33]	392.28 <sup>1</sup> 400.98 <sup>2</sup> 401.19 <sup>3</sup>	411.2[23]
Kr <sup>+22</sup> (Si-like)	3p <sup>2</sup> <sup>3</sup> P <sub>1</sub> – <sup>3</sup> P <sub>2</sub>	384.1146±0.0003	384.26[23] 384.09±0.03[31]	367.56 <sup>1</sup> 382.43 <sup>2</sup> 383.43 <sup>3</sup>	384.5[23] 383.2[20]

<sup>1</sup> Calculation using zero order approximation.

<sup>2</sup> Calculation including valence-shell correlation.

<sup>3</sup> Calculation including core-valence and core-core correlation.

\* A recent independent measurement.

Table 2: The list of the results of this work and other works, for both experiments and theories.

Therefore, we performed a completely independent measurement for Ar<sup>13+</sup> after the Fre-EBIT had been moved to Heidelberg. The two results from our independent measurements agree with each other within error bars.

The theoretical results are mostly two or three orders of magnitudes lower in accuracy compared to those achieved in this experiment; see Table 2. It is obvious that the semi-empirical calculations are in better agreement with our result. The wavelengths predicted by Kaufman et al. [20], are 0.012 nm and 0.9 nm away from our experimental results for Ar<sup>9+</sup> and Kr<sup>22+</sup>, respectively. The predictions by Edlén for Ar<sup>10+</sup>, Ar<sup>13+</sup>, and Ar<sup>14+</sup>, are 0.09 nm, 0.06 nm and 0.02 nm, respectively, different from our experimental wavelengths. The situations for *ab initio* calculations are less satisfying, usually several tens of nm away from our experimental results. The closest wavelength, from MCDF calculation by Das et al. is 0.06 nm different from our result of Ar<sup>13+</sup>. From our MCDF calculations one can see that taking into account the core-valence and core-core correlations does improve the

theoretical value, even though the final results are still not satisfying.

#### 4. CONCLUSION

In conclusion, the highly precise experimental wavelengths of ground configuration M1 transitions of highly charged Ar and Kr ions were obtained in this work. The accuracy reached up to the 0.23 ppm level, 30 times higher than the previous record for this kind of transitions. Discrepancies between *ab initio* calculations and experimental results are revealed, thus, calling on refined higher accurate modern atomic structure calculations.

We would like to thank Prof. V. P. Shevelko, Prof. I. Martinson, Dr. R. Hutton, and Dr. S. Hultdt for helpful discussions. We gratefully acknowledge support from the Leibniz-Programm as well as from the separate funding contract (ULL 166/2-1) of the Deutsche Forschungsgemeinschaft, from the Max-Planck-Institut für Kernphysik

in Heidelberg, from the Deutsche Hochschulbauförderung and from the University of Freiburg.

## REFERENCES

- [1] J. N. Lockyer, in *Dawn of Astronomy*, (1894), (reprint MIT Press), 1964.
- [2] R. W. P. McWhirter and H. P. Summers, *App. At. Coll. Phys.*, Vol.2, pp. 51, 1984.
- [3] A. H. Gabriel and C. Jordan, in *Case Studies in Atomic Collisions Physics*, edited by E. W. McDaniel and M. C. R. McDowell, (North Holland Press 1985), Vol. 2, pp. 209.
- [4] B. Edlén, *Z. Astrophys.* Vol. 55, pp.30, 1942.
- [5] I. Martinson, J. O. Ekberg and U. Litzen, *Comments At. Mol. Phys.*, Vol. 31, pp. 1, 1995.
- [6] K. N. Huang, Y. K. Kim, K. T. Cheng and J. P. Desclaus, *Phys. Rev. Lett.* Vol. 48, pp. 1245, 1982.
- [7] D. P. Das, J. Hata and I. P. Grant, *J. Phys. B* Vol. 17, pp. L1, 1984.
- [8] M. S. Safronova, W. R. Johnson and U. I. Safronova, *Phys. Rev. A* Vol. 54, pp. 2850, 1996.
- [9] M. K. Aly, in *The Solar Corona*, edited by J.W. Evans (Academic Press, New York, 1963).
- [10] A. K. Bathia, U. Feldmann and J. F. Seely, *At. Data Nucl. Data Tab.*, Vol. 35, pp. 453, 1996.
- [11] M. S. Safronova, W. R. Johnson and J. F. Safronova, *Phys. Rev. A*, Vol 53, pp. 4036, 1996.
- [12] B. Edlen, *Phys. Scr.*, Vol. 28, pp. 438, 1983.
- [13] J. Gillaspay, in *Trapping Highly Charged Ions: Fundamentals and Applications*, (NOVA Science Publishers Inc., New York, 2001).
- [14] B. Edlén, *Phys. Scr.* Vol. 26, pp. 71, 1982.
- [15] B. Edlen, *Phys. Scr.* Vol. 28, pp. 51, 1983.
- [16] D. J. Bieber, H. S. Margolis, P. K. Oxley and J. D. Silver, *Phys. Scr.* Vol. T73, pp. 64, 1997.
- [17] T. Shirai, K. Okazaki and J. Sugar, *J. Phys. Chem. Ref. Data*, Vol. 24, pp. 1577, 1995.
- [18] T. Shirai at el., *Phys. Scr.*, Vol. 58, pp. 597, 1998.
- [19] F. G. Serpa at el., *Phys. Rev. A*, Vol. 55, pp. 597, 1997.
- [20] V. Kaufman and J. Sugar, *J. Phys. Chem. Ref. Data*, Vol. 15, pp. 321, 1986.
- [21] K. T. Cheng, Y. K. Kim and J. Desclaus, *At. Data Nucl. Data Tab.*, Vol. 24, pp. 111, 1979.
- [22] K. Butler and C. J. Zeippen, *Astrophys. Supp. Ser.*, Vol. 108, pp. 1, 1994.
- [23] J. R. Crespo Lopez Urrutia, P. Breisdorfer, K. Widmann and V. Decaus, *Phys. Scr.*, Vol. T80, pp. 448, 1999.
- [24] J. T. Jefferies, *Mem. Soc. R. Sci. Liege Vol. Vol. 17*, pp. 213, 1969.
- [25] G. Wlerick and C. Fehrenbach, in *The Solar Corona*, edited by J.W. Evans (Academic Press, New York, 1963).
- [26] G. M. Nikolsky, R. A. Gulyaev and K. I. Nikolskaya, *Solar Phys.*, Vol. 21, pp. 332, 1971.
- [27] B. Lyot and A. Dollfus, *C. R. Acad. Sci. Paris*, Vol. 237, pp. 855, 1953.
- [28] M. H. Prior, *J. Opt. Soc. Am. B*, Vol 4, pp 144, 1987.
- [29] C. A. Morgan at el., *Phys. Rev. Lett.*, Vol. 74, pp. 1716, 1995.
- [30] J. R. Crespo López-Urrutia, P. Beiersdorfer, K. Widmann and V. Decaus, in *Scientific Program and Abstracts of Contributed papers of the Nineteenth International Conference on the Physics of Electronic and Atomic Collisions, Whistler, 1995*, edited by. J. B. A. Mitchell, J. McConkey and C. E. Brion, 1995, Vol. 2, pp. 589.
- [31] [31] J. R. Roberts, T. Pittman, J. Sugar, and V Kaufman, *Phys. Rev. A*, Vol. 35, pp. 2591, 1987.
- [32] [32] A. Träbert, S. B. Utter, P. Beiersdorfer, *Phys. Lett. A*, Vol. 272, pp. 86, 2000.
- [33] [33] A. Träbert, P. Beiersdorfer, G. V. Chen, D. B. Thorn and E. Biemont, *Phys. Rev. A*, Vol. 64, 042511, 2001.
- [34] [34] C. Z. Dong, S. Fritzsche, B. Fricke and W. D. Sepp, *Phys. Scr.*, Vol. T92, pp. 294, 2001.

**Sadržaj** – U radu su predstavljene rezultati eksperimentalnog izučavanja magnetnih dipolnih prelaza (M1) kod visoko naelektrisanih jona argona ( Ar X, Ar XI, Ar XIV, Ar XV) i kriptonu (Kr XIX, Kr XXIII). Talasne dužine ovih zabranjenih prelaza u vidljivoj i bliskoj ultravioletnoj oblasti određene su sa neprvidenom tačnošću do nivoa sub ppm koristeći EBIT (Electron Beam Ion trap) kao pogodan jonski izvor. Naša merenja talasnih dužina predstavljaju referentne tačke i izazov za svaremenu teoriju strukture atoma.

### PRECIZNA MERENJA TALASNIH DUŽINA ZABRANJENIH PRELAZA KOD VISOKO NAELEKTRISANIH JONA ARGONA I KRIP-TONA

Ilija N. Draganić, Jose R. Crespo López-Urrutia, Rosario Soria, Robert DuBois, Stephan Fritzsche, Yaming Zou i Joachim Ullrich